Available online at www.sciencedirect.com

SciVerse ScienceDirect

Ceramics International 38 (2012) 4151–4158

CERAMICS INTERNATIONAL

www.elsevier.com/locate/ceramint

Structural, optical and methanol sensing properties of sprayed In_2O_3 nanoparticle thin films

N.G. Pramod, S.N. Pandey, P.P. Sahay *

Department of Physics, Motilal Nehru National Institute of Technology, Allahabad 211 004, India

Received 5 December 2011; received in revised form 26 December 2011; accepted 26 January 2012
Available online 4 February 2012

Abstract

Indium oxide (In_2O_3) nanoparticle thin films were grown on cleaned glass substrates by the chemical spray pyrolysis technique using the precursor solution of indium nitrate (In $(NO_3)_3$). The XRD studies confirm that the films are polycrystalline In_2O_3, possessing cubic structure with lattice parameters, $a = b = c = 10.17$ Å. The optical studies show a direct optical band gap of 3.32 eV and an indirect band gap of 2.6 eV in the prepared films. The films exhibit high optical transparency >80% in the visible region, reaching a maximum of 85% at 684 nm wavelength. Further, the gas sensing properties of the films have been investigated for various concentrations of methanol in air at different operating temperatures. At 300 °C the film exhibits a very high response 99% to methanol vapor at a concentration of 40 ppm in air, which is ideal to be used as a methanol sensor. The film shows fast response and recovery to methanol vapor at higher operating temperatures. A possible methanol sensing mechanism has been proposed.

Keywords: C. Optical properties; In_2O_3 nanoparticle thin films; Spray pyrolysis; Methanol sensor

1. Introduction

Among the available transparent conducting oxides (TCOs), indium oxide (In_2O_3), an n-type semiconductor, is a promising candidate for use in various optoelectronic devices and solar cells owing to its good optical transparency in the visible region (>80%) and low electrical resistivity ($\sim 10^{-4}\ \Omega$ m) [1,2]. Furthermore, In_2O_3, both in bulk and thin film form, has been used as a sensor for various gases such as volatile organic compounds (VOCs), Cl_2, NO_2, humidity, etc. [3]. Since the gas sensing properties of materials are the surface phenomena, therefore thin films are more suitable as compared to the bulk counterparts [4]. Many deposition techniques have been employed to prepare thin films of In_2O_3. These include sol–gel process, spray pyrolysis, thermal evaporation, pulsed laser deposition, etc. For the growth of indium oxide thin films by spray pyrolysis technique, in most cases indium chloride ($InCl_3$) has been used as the starting material [5–12] whereas in few cases indium nitrate (In $(NO_3)_3$) has been used to serve the purpose [13,14].

Methanol is a widely used organic solvent for a variety of purposes. It is used as fuel, antifreeze and laboratory solvent. Since methanol is highly toxic in nature, it is very important to detect its vapor at very low concentrations. Among the VOCs for gas sensor applications, methanol is a less studied organic compound as compared to ethanol and acetone. Hence, there is a need for development of reliable sensors capable of detecting methanol vapor in air. A number of metal oxides have been studied for their methanol sensing properties by various researchers. Patel et al. [15] have reported response of the methanol vapor on the indium tin oxide thin films. CeO_2–Fe_2O_3 thin films as the methanol sensor have been studied by Neri et al. [16]. Sahay et al. [17] have investigated the methanol sensor response of the Al-doped ZnO thin films. Sol gel derived SnO_2 films have been examined for their methanol sensing properties by Teeramongkonrasmee et al. [18].

Gas sensors based on the indium oxide thin films have been reported in the literature. Tamaki et al. [19] have reported the chlorine sensing properties of the In_2O_3 thin films prepared by the electron beam evaporation technique. Chung et al. [20] have grown the indium oxide thin films on silicon and alumina

* Corresponding author. Tel.: +91 532 2271260; fax: +91 532 2545341.
E-mail address: dr_ppsahay@rediffmail.com (P.P. Sahay).

0272-8842/$36.00
doi:10.1016/j.ceramint.2012.01.075

substrates and discussed their CO, H_2 and C_3H_8 sensing properties. Low temperature indium oxide sensors have been fabricated by Winter et al. [21] using molecular beam epitaxy technique, and the films show significant response for a number of gases including NH_3 and NO_2. Indium oxide films have been examined for detection of ozone gas by Suchea et al. [22].

To the best of our knowledge, the methanol sensing properties of the In_2O_3 thin films grown by the spray pyrolysis technique have not been reported till date. Therefore, in the present investigation, the In_2O_3 thin films have been grown by the chemical spray pyrolysis technique using the precursor solution of $In(NO_3)_3$. Studies on the methanol gas sensing properties of the films have been carried out at low operating temperatures and for low concentrations. Further, the as-grown films have undergone optical characterization and a number of optical constants which include refractive index, optical band gaps, etc. have been determined.

2. Experimental details

In_2O_3 films have been deposited on cleaned glass substrates by employing the spray pyrolysis technique. Indium nitrate ($In(NO_3)_3$), 99.98% pure (Sigma Aldrich), was used as the precursor and distilled water as the solvent. The glass substrates were cleaned prior to deposition, firstly by freshly prepared chromic acid followed by deionized water, and then ultrasonically cleaned by trichloroethylene for about 30 min. After this, they were washed with deionized water again and finally dried in air. A schematic representation of the spray apparatus has been described elsewhere [4]. The precursor solution was sprayed through a locally designed glass nozzle on the hot substrates with pressurized air being the carrier gas. The various process parameters for the film deposition are listed in Table 1. The thickness of the resulting films prepared by spraying 3 ml of the 0.1 M indium nitrate solution was estimated by weight-difference method. The films thus prepared were subjected to structural, optical, electrical and methanol sensing studies.

Structural analyses of the films were carried out using PANalytical X'Pert PRO with CuKα radiation (λ = 1.5406 Å) as the X-ray source at 30 mA, 30 kV, the scanning angle 2θ varying from 20° to 65° at a scan speed of 0.02° per second. In order to determine the band structure and energy band gap, the optical studies of the indium oxide films were carried out using Perkin Elmer Lambda 35 UV–vis spectrometer (UK) in the spectral range 300–700 nm. For electrical measurements, high conducting silver paste was applied on both ends of the films for making ohmic contacts. The methanol sensing properties of the film were carried out in an experimental set up shown in Fig. 1. The film was mounted on a two-probe assembly placed into a silica tube, which was inserted coaxially inside a resistance-heated furnace. The electrical resistance of the films was measured before and after exposure to methanol vapor using a Keithley System Electrometer model 6517B. The measurement of methanol concentration was carried out by taking required amount of liquid methanol in a Hamilton micro syringe and then injecting it into the glass tube, as shown in Fig. 1. The response to methanol of the film was determined at different operating temperatures in the range 200–300 °C for various concentrations of methanol in air.

Table 1
Process parameters for the spray deposition of the In_2O_3 thin films.

Spray process parameters	Optimum value/item
Substrate temperature	400 ± 10 °C
Solvent	Deionised water
Substrate	Glass
Substrate-nozzle distance	15 cm
Carrier gas pressure	3 kg/cm^2
Solution flow rate	3 ml/min
Solution concentration	0.1 M

3. Results and discussion

3.1. Film formation

It is well known that the physical, optical and structural properties of a film are strongly affected by many growth parameters during its formation [23]. In the chemical spray pyrolysis technique, when aerosol droplets of required solution arrive close to the heated glass substrates, a pyrolytic decomposition process takes place and a highly adherent desired film is formed on the substrates. A possible reaction mechanism in the formation of In_2O_3 film is as follows:

$$In(NO_3)_3 + H_2O \rightarrow In_2O_3 + HNO_3 \uparrow \quad (1)$$

The films thus prepared were found to be almost clear and pale yellow in color in physical appearance. All the film thicknesses were found to be in the range 200–250 nm.

3.2. Structural analyses

The X-ray diffraction spectra of the In_2O_3 thin film is shown in Fig. 2. The observed XRD pattern is found to match with the JCPDS card 06-0416. All the films are found to have polycrystalline nature, possessing cubic structure with lattice parameters, $a = b = c = 10.17$ Å which is slightly greater than the reported value of 10.118 Å for pure indium oxide [24]. This change in the value of lattice parameter may be attributed to the oxygen deficiency and the strain effect arising from thermal expansion coefficient and a lattice mismatch between the film and the substrate [25].

The lattice parameters ($a = b = c$) have been determined by equation [26]:

$$d = \frac{a}{\sqrt{h^2 + k^2 + l^2}} \quad (2)$$

where d is the lattice spacing of the crystal planes ($h\ k\ l$).

The crystallite size (D) has been determined from the full width at half maximum (FWHM) of the different XRD peaks, using the Scherrer formula [27]:

$$D = \frac{k\lambda}{B\cos\theta} \quad (3)$$

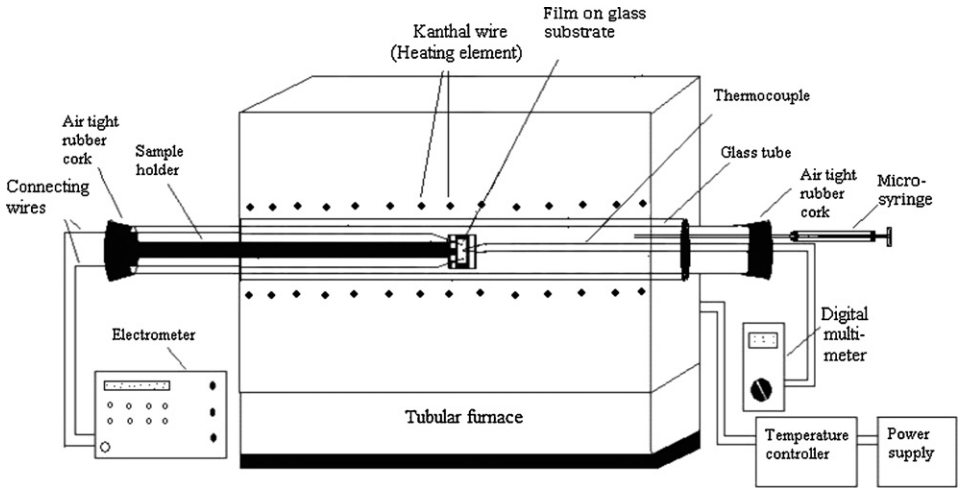

Fig. 1. Experimental set up for methanol sensing studies.

where k is the shape factor possessing a numerical value of 0.9, λ is the wavelength of the X-ray, θ is the Bragg's angle and B is the corrected FWHM in radians for instrumental broadening. The average crystallite size has been found to be ~19 nm.

The lattice strain (ε) has been determined using the tangent formula [27]:

$$\varepsilon = \frac{B}{4\tan\theta} \tag{4}$$

The XRD peak position, the lattice d-spacing, the crystallite size and the lattice strain of the film thus obtained are listed in Table 2.

3.3. Optical studies

The transmittance and absorbance spectra of the film are shown in Fig. 3. The film shows a high optical transparency greater than 80% in the visible region, the value of transmittance reaching a maximum of 85% at 684 nm wavelength. We have calculated a number of optical constants

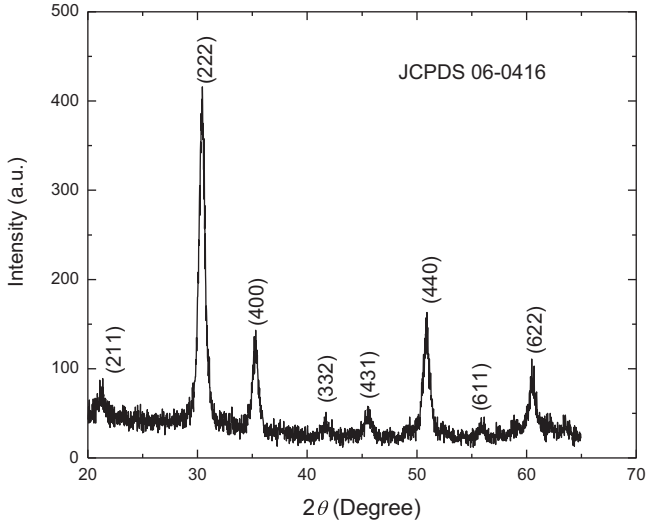

Fig. 2. XRD spectra of the In_2O_3 nanoparticle thin film.

based on the analysis of the data retrieved. This includes (i) the values of optical band gap for direct and indirect transitions, (ii) the width of the localized states near the conduction band, and (iii) the refractive index, n.

The optical band gap has been calculated for both direct and indirect transitions as indium oxide is reported to have both these values because light is absorbed by both direct and indirect interband transitions in this oxide material [28,29]. For allowed electronic transition in materials, the absorption coefficient α is given by equation [23]:

$$\alpha h\nu = K(h\nu - E_g)^p \tag{5}$$

where p has discrete values like 1/2, 3/2, 2, or more depending on whether the transition is direct or indirect, and allowed or forbidden. In the direct and allowed cases, p = 1/2 whereas for direct but forbidden cases it is 3/2. But for the indirect and allowed cases p = 2 and for the forbidden cases it will be 3 or more. K is a constant given by equation [23]:

$$K = \left[\frac{e^2}{(\pi n c m_e^* h^2)}\right](2m_r)^{3/2} \tag{6}$$

where m_e^* and m_r are the effective and reduced masses of charge carriers, respectively. E_g is the optical bandgap. Thus, a plot between $(Ah\nu)^{1/2}$ vs. $h\nu$ (shown in Fig. 4) gives us the value of the indirect band gap, E_g which is obtained by extrapolating the linear portion of the plot to the energy axis. The indirect band gap thus obtained has been found to be 2.6 eV.

For direct band gap estimation, a graph is plotted between $(Ah\nu)^2$ vs. $h\nu$, as shown in Fig. 5. On extrapolating the linear portion of the plot to the energy axis, the direct band gap has been found to be 3.32 eV, which is slightly lower than the values reported in the literatures [30–33]. This may be due to the formation of some localized states near the conduction band during the film growth process, as there is lattice strain due to lattice mismatch between the crystalline indium oxide film and the amorphous glass substrate. Such a study of calculating direct and indirect band gaps for the indium oxide thin films has

Table 2
Structural parameters of the In_2O_3 thin film.

2θ (in degrees)	d-spacing (JCPDS) (Å)	d-spacing observed (Å)	(h k l)	Lattice parameters a = b = c (Å)	Crystallite size (nm)	Lattice strain (%)
21.2139	4.1300	4.1882	211	10.2591	12.83	0.00051
30.46	2.9210	2.9347	222	10.1662	20.92	0.00046
35.3012	2.5290	2.5425	400	10.1703	26.47	0.00043
41.7187	2.1570	2.1651	332	10.1552	18.00	0.00078
45.4829	1.9840	1.9942	431	10.1689	18.24	0.00086
50.8827	1.7880	1.7946	440	10.1518	22.35	0.00081
55.872	1.6410	1.6456	611	10.1442	14.28	0.00145
60.4769	1.5250	1.5295	622	10.1461	19.16	0.00122

Table 3
Response of methanol sensors based on various oxide thin films.

Sensing element	Deposition technique; material/precursor used	Operating temperature (°C)	Formula used for response calculation	Response for methanol vapor	Reference
In_2O_3 thin film	Spray pyrolysis; In $(NO_3)_3$	300	$[(R_a - R_g)/R_a] \times 100\%$	99% for 40 ppm	This work
Al-doped ZnO thin film	Spray pyrolysis [Zn $(CH_3COOH)_2$]. $2H_2O$ (host precursor) + $AlCl_3$ (dopant precursor)	275	$[(R_a - R_g)/R_a] \times 100\%$	44% for 500 ppm	[17]
SnO_2 thin film	$SnCl_4$ + NaOEt	230	R_a/R_g	23% for 10,000 ppm	[18]
Pd-gate MOS	MOS structure on p-type Si substrate	120	$(\Delta C/C_a) \times 100$, where C is the capacitance	57% for 35,000 ppm	[35]
In_2O_3/SnO_2 thin film	Direct evaporation technique;ITO (In_2O_3+ 17% SnO_2)	350	$(G_g - G_a)/G_a$, where G is the conductance	0.03; concentration not specified.	[36]
CeO_2–Fe_2O_3 thin film	Liquid phase method; $CeCl_3.7H_2O$ and $Fe(NO_3)_3.9H_2O$	475	I_g/I_a, where I is the current	11% for 200 ppm	[16]

been reported by Girtan, and the values are found to be 3.57–3.68 eV and 2.8–3.2 eV, respectively [6].

The absorption coefficient α in the low energy range follows the well-known exponential law, that is, the Urbach tail expressed as [34]:

$$\alpha = \alpha_o \exp\left(\frac{h\nu}{E_o}\right) \quad (7)$$

where α_o is a constant and E_o is a parameter describing the width of the tail of localized states in the band gap. In terms of absorption, Eq. (7) can be written as

$$A = A_o \exp\left(\frac{h\nu}{E_o}\right) \quad (8)$$

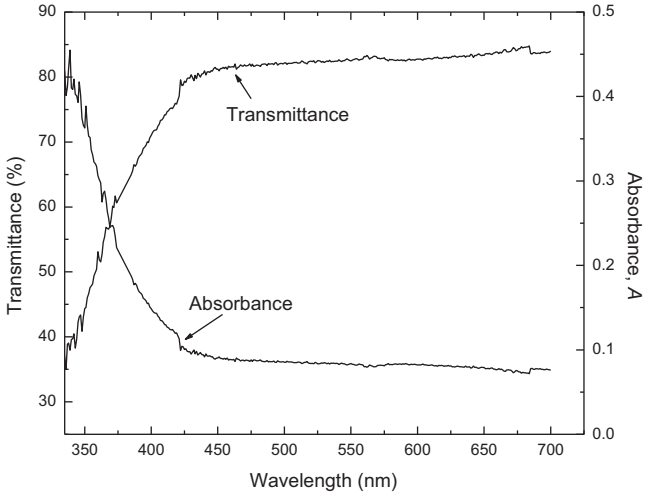

Fig. 3. Transmittance and absorbance spectra of the In_2O_3 thin film as a function of wavelength.

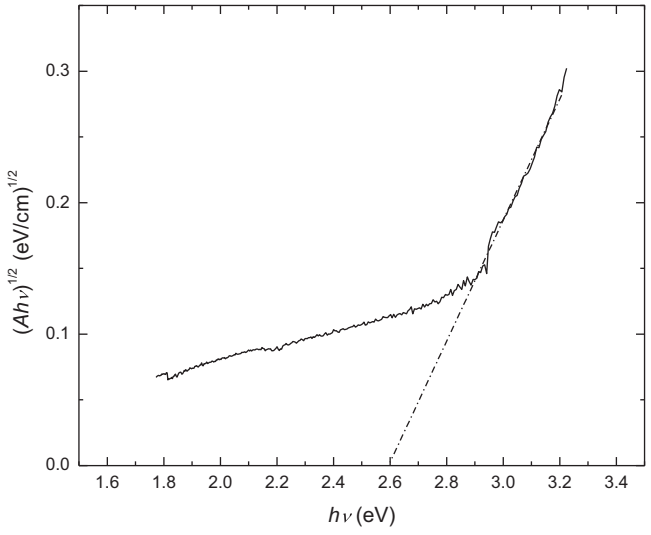

Fig. 4. Variation of $(Ah\nu)^{1/2}$ vs. $h\nu$ for the In_2O_3 thin film.

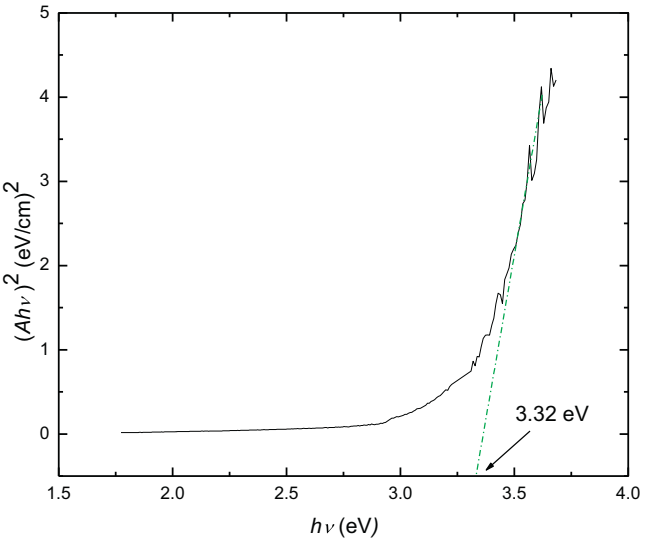

Fig. 5. Variation of $(Ah\nu)^2$ vs. $h\nu$ for In_2O_3 thin film.

where A_o is another constant. E_o has been estimated, from the slope of the linear relationship ln A against $h\nu$ (shown in Fig. 6), to be 0.503 eV.

The refractive index, n of the film is determined using the relation [23]:

$$R = \frac{(n-1)^2}{(n+1)^2} \tag{9}$$

where R is the normal reflectance. This relation is valid for the case when the absorption is very low. In the present case, the refractive index at 550 nm is found to be 2.13 which is close to the results observed in the case of the pulsed laser ablated nanostructured indium oxide thin films [1,30]. The variation of refractive index, n in the wavelength range 500–600 nm is shown in Fig. 7.

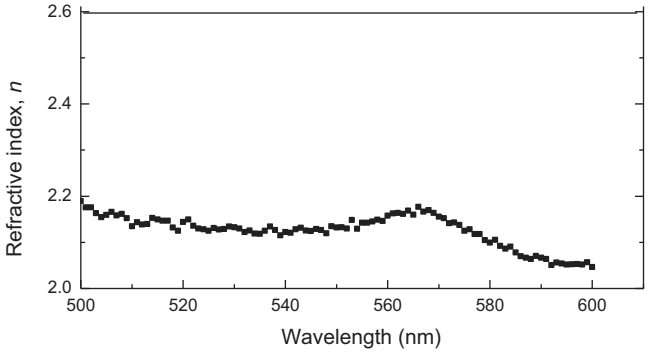

Fig. 7. Variation of refractive index, n with wavelength.

3.4. Electrical studies

The variation of electrical resistance of the In_2O_3 film as a function of temperature is shown in Fig. 8. It is observed that the resistance of the film first increases with temperature up to 75 °C, which may be attributed to the adsorption of atmospheric oxygen on the film surface. On further increasing the temperature, the resistance begins to fall. In the temperature range 125–200 °C, the film resistance decreases rapidly with rise in temperature, while decrease in resistance is slower in the temperature range 200–300 °C. In fact, two competing processes of thermal excitation of electrons and oxygen adsorption occur simultaneously. The sharp reduction in film resistance in the temperature range 125–200 °C is because the thermal excitation of electrons dominates over the oxygen adsorption process, while the gradual decrease in the film resistance with temperature in the range 200–300 °C may be the result of improved adsorption of atmospheric oxygen at higher temperatures. Dependence of the electrical conductivity of the film on temperature is shown in Fig. 9.

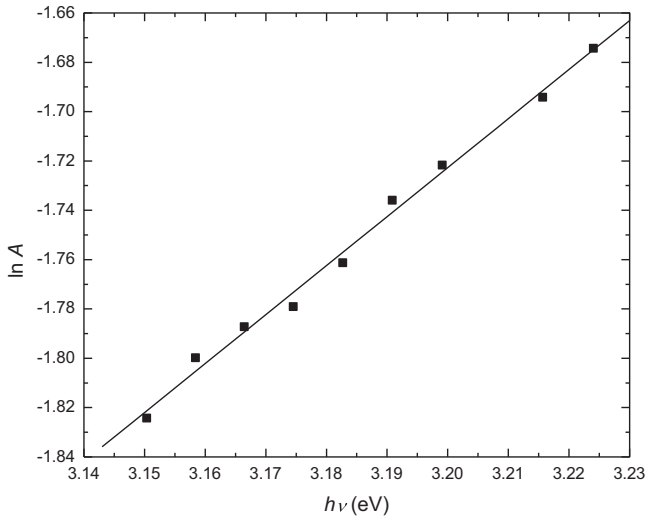

Fig. 6. Variation of ln A with $h\nu$.

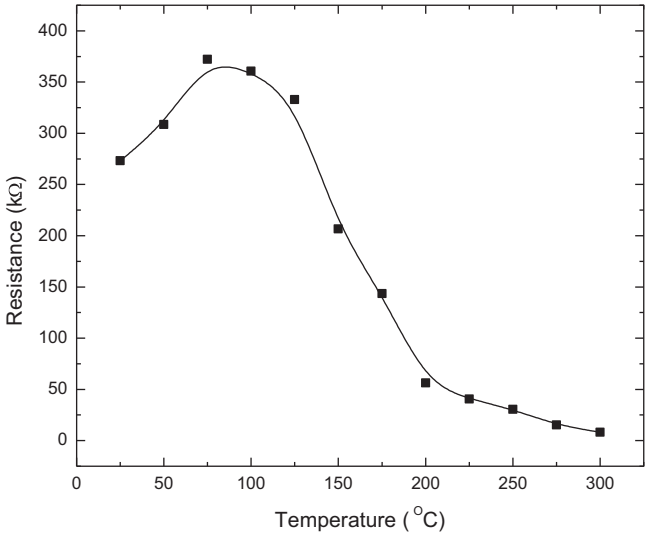

Fig. 8. Variation of electrical resistance of the In_2O_3 thin film as a function of temperature.

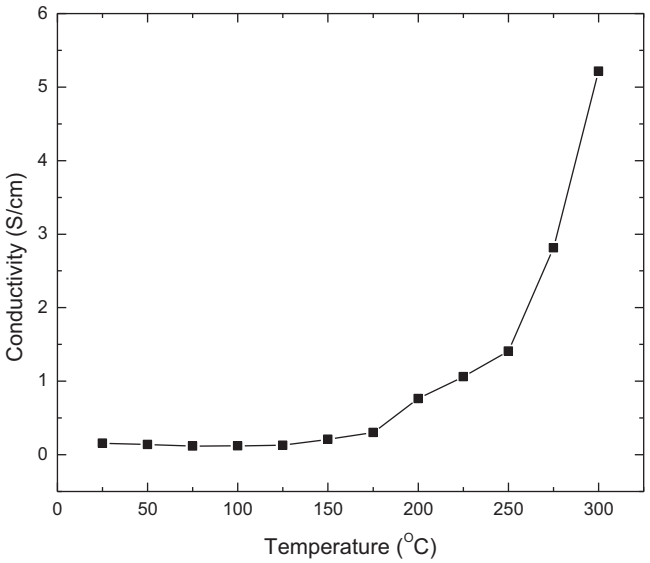

Fig. 9. Dependence of electrical conductivity of the film on temperature.

3.5. Methanol-sensing studies

The electrical resistance of the film decreases upon exposure to methanol being a reducing gas, and it increases under recovering in air. The sensor response has been defined as $[((R_a - R_g)/R_a) \times 100\%]$. Here, R_a is the resistance of the film in air and R_g is the resistance upon exposure to methanol.

Fig. 10 presents the response characteristics of the film as a function of operating temperature for different concentrations of methanol in air. Below the operating temperature of 200 °C, the response of the film is found to be very low. This is because the response of the film to methanol vapor is restricted by the speed of the chemical reaction. At low temperatures, the methanol molecules do not have enough thermal energy to react with the surface adsorbed oxygen species. When the film is heated beyond 200 °C, the methanol molecules have enough thermal energy to react with the surface adsorbed oxygen species, thus releasing electrons to the conduction band. This, in turn, reduces the film resistance and therefore increases the sensor response. It is observed that a small increase in the operating temperature from 200 °C to 225 °C, leads to a large increase in the sensor response because of the availability of sufficient adsorbed oxygen species on the film surface. The film shows maximum response (99%) at 300 °C for 40 ppm concentration of methanol in air. It is seen that beyond 225 °C, the increase in response with operating temperature is not so rapid as compared to the response observed in the temperature range 200–225 °C for all concentrations of methanol in air. This may be due to a decrease in the reaction kinetics of methanol molecules with the adsorbed oxygen species on the film surface.

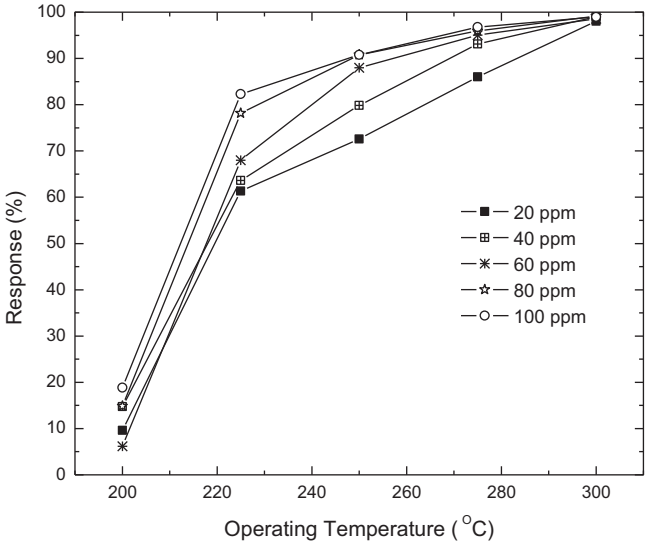

Fig. 10. Methanol response characteristics of the In_2O_3 thin film as a function of operating temperature.

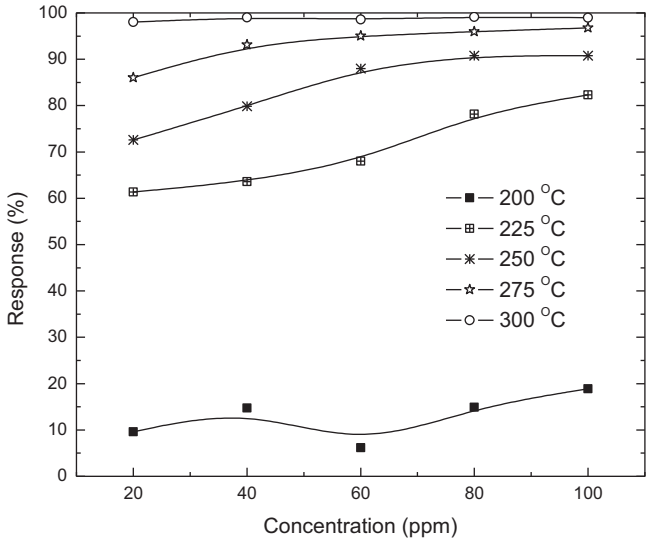

Fig. 11. Response characteristics of the In_2O_3 thin film as a function of methanol concentration at different operating temperatures.

Fig. 11 shows the response characteristics of the film as a function of methanol concentration at different operating temperatures. At 200 °C, because the thermal energy is low, a concentration as high as 100 ppm does not contribute much for the sensor response. It is observed that at 225 °C, the response increases gradually with methanol concentration. However, at the operating temperatures of 250 °C and beyond, the response first increases gradually with concentration up to 80 ppm and thereafter tends to attain saturation. This gradual increase in response with methanol concentration is attributed to the fact that the surface coverage of methanol molecules begins to attain saturation with increase in methanol concentration. At 300 °C, the film shows a high response of 98% even at a low concentration of 20 ppm of methanol in air. This suggests that at 300 °C and 20 ppm concentration, the methanol molecules cover a large surface area of the film, which reacts very effectively with the adsorbed oxygen species.

Fig. 12(a) and (b) presents the transient response characteristics of the indium oxide film for various concentrations of methanol in air at two different operating temperatures 250 °C

and 300 °C, respectively. It is observed that at 250 °C, the response and recovery is the fastest for 80 ppm as compared to other concentrations. At 250 °C, for lower concentrations of methanol, the response time of the film is found to be large as compared to that for higher concentrations. However, the case is reversed for recovery time, i.e., the recovery time is short for lower concentrations and long for higher concentrations of methanol in air. Longer response time observed in case of lower concentrations may be due to sparse coverage of methanol molecules on the film surface.

At 300 °C, the film shows fast response at all concentrations, which is possibly due to fast reaction kinetics of the methanol molecules with the adsorbed oxygen species at 300 °C, whereas the recovery time is found to increase with the methanol concentration in air.

The sensing mechanism of methanol to In_2O_3 thin film is a surface controlled phenomenon. At first, oxygen is chemisorbed on the indium oxide surface when the film is heated in air. During the chemisorption process, atmospheric oxygen O_2 is converted into its ionic species viz. O_2^- and O^- which acquire electrons from the conduction band. The reaction kinetics is as follows [17]:

$$O_2\,(\text{air}) \leftrightarrow O_2\,(\text{ads}) \tag{10}$$

$$O_2\,(\text{ads}) + e^- \leftrightarrow O_2^-\,(\text{ads}) \tag{11}$$

$$O_2^-\,(\text{ads}) + e^- \leftrightarrow 2O^-\,(\text{ads}) \tag{12}$$

The reaction between methanol vapor and adsorbed ionic oxygen species can take place by two different ways [17]:

$$CH_3OH\,(\text{gas}) + O^-\,(\text{ads}) \rightarrow HCOH + H_2O + e^- \tag{13}$$

$$HCOH + O\,(\text{bulk}) \rightarrow HCOOH + O\,(\text{vacancies}) \tag{14}$$

$$CH_3OH\,(\text{gas}) + O_2^-\,(\text{ads}) \rightarrow HCOOH + H_2O + e^- \tag{15}$$

Thus, once the film is exposed to the methanol vapor, the formation of formaldehyde and formic acid by the oxidation of methanol, leads to the liberation of electrons into the conduction band, resulting a decrease in the film resistance.

A comparison of this work with other methanol sensors fabricated using various metal oxide semiconductors is presented in Table 3. It is inferred from the comparison that In_2O_3 is a better material for detection of the methanol vapor. Thus, for the detection of low concentration of methanol, the In_2O_3 thin film grown by the spray pyrolysis technique is a promising candidate to serve as a methanol sensor.

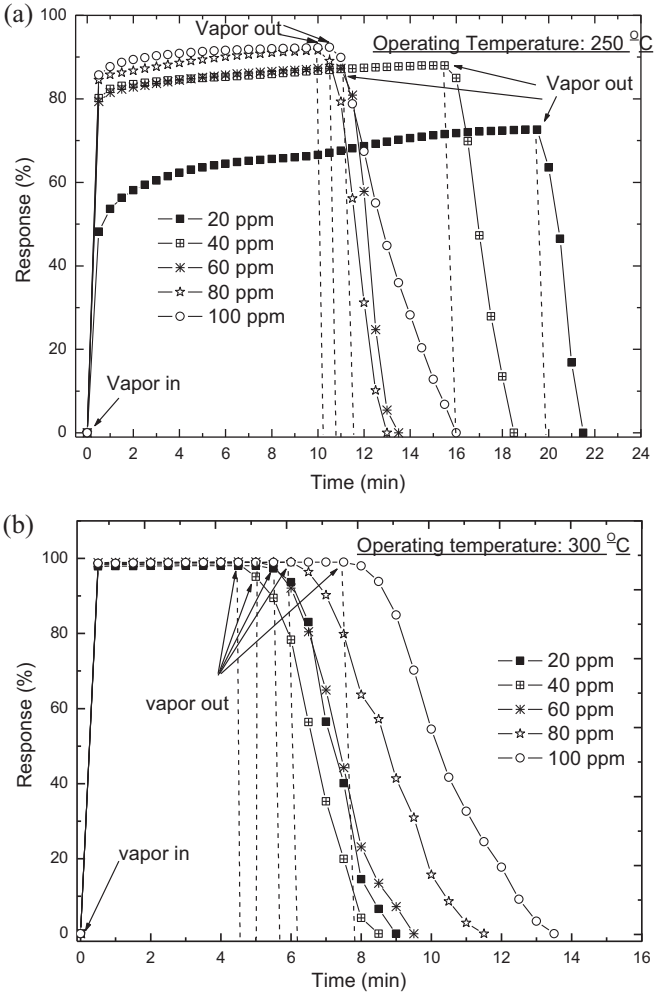

Fig. 12. (a) and (b) Transient response characteristics of the In_2O_3 thin film at two different operating temperatures (a) 250 °C and (b) 300 °C.

4. Conclusions

(i) The indium oxide nanoparticle thin films prepared by the pyrolytic decomposition of the aqueous solution of indium nitrate are found to have cubic structure with crystallite size ∼19 nm.

(ii) A high optical transparency greater than 80% in the visible region has been observed for the films under study. Direct and indirect optical band gaps have been found to be 3.32 eV and 2.6 eV, respectively. The width of the localized states below the conduction band has been estimated to be 0.503 eV. The refractive index has been calculated to be 2.13 at 550 nm wavelength.

(iii) The change in the film resistance as a function of operating temperatures has been explained by two competing processes, viz. the thermal excitation of electrons and the atmospheric oxygen adsorption, occurring simultaneously.

(iv) The response to methanol vapor is found to be maximum (99%) at 300 °C for a concentration of 40 ppm in air. The maximum response is attributed to the availability of sufficient adsorbed ionic species of oxygen on the film surface, which react most effectively with the methanol molecules at this particular temperature.

(v) The reaction mechanism of methanol sensing has been explained.

Acknowledgments

The authors are thankful to National Centre for Experimental Mineralogy and Petrology, University of Allahabad,

India for providing XRD facilities. They are grateful to the Department of Science & Technology, Govt. of India, for providing financial support under research project (No. SR/S2/CMP-41/2008).

References

[1] D. Beena, K.J. Lethy, R. Vinodkumar, A.P. Detty, V.P. Mahadevan Pillai, V. Ganesan, Photoluminescence in laser ablated nanostructured indium oxide thin films, J. Alloys Compd. 489 (2010) 215–223.

[2] P.K. Manoj, K.G. Gopachandran, P. Koshy, V.K. Vaidyan, B. Joseph, Growth and characterization of indium oxide thin films prepared by spray pyrloysis, Opt. Mater. 28 (2006) 1405–1411.

[3] G. Korotcenkov, Metal oxides for solid-state gas sensors: what determines our choice? Mater. Sci. Eng. B 139 (2007) 1–23.

[4] C.S. Prajapati, S.N. Pandey, P.P. Sahay, Sensing of LPG with nanostructured zinc oxide thin films grown by spray pyrolysis technique, Physica B 406 (13) (2011) 2684–2688.

[5] S.M. Rozati, T. Ganj, Transparent conductive Sn-doped indium oxide thin films deposited by spray pyrolysis technique, Renew. Energy 29 (2004) 1671–1676.

[6] M. Girtan, Investigations on the optical constants of indium oxide thin films prepared by ultrasonic spray pyrolysis, Mater. Sci. Eng. B 118 (2005) 175–178.

[7] G. Korotcenkov, M. Nazarov, M.V. Zamoryanskaya, M. Ivanov, Cathodoluminescence emission study of nanocrystalline indium oxide films deposited by spray pyrolysis, Thin Solid Films 515 (2007) 8065–8071.

[8] V. Brinzari, G. Korotcenkov, V. Matolin, Synchrotron radiation photoemission study of indium oxide surface prepared by spray pyrolysis method, Appl. Surf. Sci. 243 (2005) 335–344.

[9] J. Joseph Prince, S. Ramamurthy, B. Subramanian, C. Sanjeeviraja, M. Jayachandran, Spray pyrolysis growth and material properties of In_2O_3 films, J. Cryst. Growth 240 (2002) 142–151.

[10] G. Korotcenkov, V. Brinzari, A. Cerneavschi, M. Ivano, A. Cornet, J. Morante, A. Cabot, J. Arbiol, In_2O_3 films deposited by spray pyrolysis: gas response to reducing (CO, H_2) gases, Sens. Actuators B 98 (2004) 122–129.

[11] P. Prathap, G. Gowri Devi, Y.P.V. Subbaiah, K.T. Ramakrishna Reddy, V. Ganesan, Growth and characterization of indium oxide films, Curr. Appl. Phys. 8 (2008) 120–127.

[12] G. Korotcenkov, V. Brinzari, A. Cerneavschi, A. Cornet, J. Morante, A. Cabot, J. Arbiol, Crystallographic characterization of In_2O_3 films deposited by spray pyrolysis, Sens. Actuators B 84 (2002) 37–42.

[13] J.-H. Lee, B.-O. Park, Transparent conducting In_2O_3 thin films prepared by ultrasonic spray pyrolysis, Surf. Coat. Technol. 184 (2004) 102–107.

[14] B.-C. Kim, J.-Y. Kim, D.-D. Lee, J.-O. Lim, J.-S. Huh, Effect of crystal structures on gas sensing properties of nanocrystalline ITO thick films, Sens. Actuators B 89 (2003) 180–186.

[15] N.G. Patel, P.D. Patel, V.S. Vaishnav, Indium tin oxide (ITO) thin film gas sensor for detection of methanol at room temperature, Sens. Actuators B 96 (2003) 180–189.

[16] G. Neri, A. Bonavita, G. Rizzo, S. Galvagno, S. Capone, P. Siciliano, Methanol gas-sensing properties of CeO_2–Fe_2O_3 thin films, Sens. Actuators B 114 (2006) 687–695.

[17] P.P. Sahay, R.K. Nath, Al-doped ZnO thin films as methanol sensors, Sens. Actuators B 134 (2008) 654–659.

[18] A. Teeramongkonrasmee, M. Sriyudthsak, Methanol and ammonia sensing characteristics of sol–gel derived thin film gas sensor, Sens. Actuators B 66 (2000) 256–259.

[19] J. Tamaki, C. Naruo, Y. Yamamoto, M. Matsuoka, Sensing properties to dilute chlorine gas of indium oxide based thin film sensors prepared by electron beam evaporation, Sens. Actuators B 83 (2002) 190–194.

[20] W.-Y. Chung, G. Sakai, K. Shimanoe, N. Miura, D.-D. Lee, N. Yamazoe, Spin-coated indium oxide thin film on alumina and silicon substrates and their gas sensing properties, Sens. Actuators B 65 (2000) 312–315.

[21] R. Winter, K. Scharnagl, A. Fuchs, T. Doll, I. Eisele, Molecular beam evaporation-grown indium oxide and indium aluminium films for low-temperature gas sensors, Sens. Actuators B 66 (2000) 85–87.

[22] M. Suchea, N. Katsaraki, S. Christoulakis, S. Nikolopoulou, G. Kiriakidis, Low temperature indium oxide gas sensors, Sens. Actuators B 118 (2006) 135–141.

[23] A. Goswami, Thin Film Fundamentals, New Age International, New Delhi, 1996.

[24] JCPDS Card no. 06-0416.

[25] X. Li, M.W. Wanlass, T.A. Gessert, K.A. Emery, T.J. Coutts, High-efficiency indium tin oxide/indium phosphide solar cells, Appl. Phys. Lett. 54 (1989) 2674.

[26] B.D. Cullity, Elements of X-ray Diffraction, Addison-Wesley, New York, 1978.

[27] H.P. Klug, L.E. Alexander, X-ray Diffraction Procedures for Polycrystalline and Amorphous Materials, Wiley, New York, 1974.

[28] A. Walsh, J.L.F. Da Silva, S.-H. Wei, C. Korber, A. Klein, L.F.J. Piper, A. DeMasi, K.E. Smith, G. Panaccione, P. Torelli, D.J. Payne, A. Bourlange, R.G. Egdell, Nature of the Band Gap of In_2O_3 Revealed by First-Principles Calculations and X-ray Spectroscopy, Phys. Rev. Lett. 100 (2008) 167402.

[29] P.D.C. King, T.D. Veal, F. Fuchs, Ch.Y. Wang, D.J. Payne, A. Bourlange, H. Zhang, G.R. Bell, V. Cimalla, O. Ambacher, R.G. Egdell, F. Bechstedt, C.F. McConville, Band gap, electronic structure, and surface electron accumulation of cubic and rhombohedral In_2O_3, Phys. Rev. B 79 (2009) 205211.

[30] D. Beena, K.J. Lethy, R. Vinodkumar, V.P. Mahadevan Pillai, V. Ganesan, D.M. Phase, S.K. Sudheer, Effect of substrate temperature on structural, optical and electrical properties of pulsed laser ablated nanostructured indium oxide films, Appl. Surf. Sci. 255 (2009) 8334–8342.

[31] B. Radha Krishna, T.K. Subramanyam, B. Srinivasulu Naidu, S. Uthanna, Effect of substrate temperature on the electrical and optical properties of dc reactive magnetron sputtered indium oxide films, Opt. Mater. 15 (2000) 217–224.

[32] M. Girtan, G. Folcher, Structural and optical properties of indium oxide thin films prepared by an ultrasonic spray CVD process, Surf. Coat. Technol. 172 (2003) 242–250.

[33] D. Beena, R. Vinodkumar, I. Navas, Geo Rajan, V.P. Mahadevan Pillai, Efficient photoluminescence from pulsed laser ablated nanostructured indium oxide films, Mater. Sci. Eng. B 174 (2010) 59–65.

[34] F. Urbach, The long-wavelength edge of photographic sensitivity and of the electronic absorption of solids, Phys. Rev. 92 (1953) 1324.

[35] P. Pandey, J.K. Srivastava, V.N. Mishra, R. Dwivedi, Pd-gate MOS sensor for detection of methanol and propanol, J. Nat. Gas Chem. 20 (2011) 123–127.

[36] V.S. Vaishnav, P.D. Patel, N.G. Patel, Preparation and characterization of indium tin oxide thin films for their application as gas sensors, Thin Solid Films 487 (2005) 277–282.